

A Challenge to Lepton Universality in B Meson Decays

Vera Lüth

the date of receipt and acceptance should be inserted later

Abstract One of the key assumptions of the Standard Model of fundamental particles is that the interactions of the charged leptons, namely electrons, muons, and taus, differ *only* because of their different masses. While precision tests have not revealed any definite violation of this assumption, recent studies of B meson decays involving the higher-mass tau lepton have resulted in observations that challenge lepton universality at the level of four standard deviations. A confirmation of these results would point to new particles or interactions, and could have profound implications for our understanding of particle physics.

Keywords Lepton universality · Flavor physics · BABAR · Belle · LHCb

Motivation

More than 70 years of particle physics research have led to an elegant and concise theory of particle interactions at the sub-nuclear level, commonly referred to as the Standard Model (SM) [1,2]. In the framework of the SM of particle physics the fundamental building blocks, quarks and leptons, are each grouped in three generations of two members each. The three charged leptons, the electron (e^-), the muon (μ^-) and the tau (τ^-) are each paired with a very low mass, electrically neutral neutrino, ν_e, ν_μ , and ν_τ . The three generations are ordered by the mass m_ℓ of the charged lepton ranging from 0.511 MeV for e^\pm to 105 MeV for μ^\pm , and 1,777 MeV for τ^\pm [3]. Charged leptons participate in electromagnetic and weak, whereas neutrinos

only undergo weak interaction. The SM assumes that these interactions of the charged and neutral leptons are universal, i.e., the same for the three generations.

Precision tests of lepton universality have been performed by many experiments. To date no definite violation of lepton universality has been observed. Among the most precise tests is a comparison of decay rates of K mesons, $K^- \rightarrow e^- \bar{\nu}_e$ versus $K^- \rightarrow \mu^- \bar{\nu}_\mu$ [4] [5]. Furthermore, taking into account precision measurements of the tau and muon masses and lifetimes, the measured decay rates $\tau^- \rightarrow e^- \bar{\nu}_e \nu_\tau$ and $\mu^- \rightarrow e^- \bar{\nu}_e \nu_\mu$, have confirmed the equality of the weak coupling strengths of the tau and muon [3].

However, recent studies of semileptonic decays of B mesons of the form $\bar{B} \rightarrow D^{(*)} \ell^- \bar{\nu}_\ell$, with $\ell = e, \mu$, or τ , have resulted in observations that seem to challenge lepton universality. These weak decays are well understood in the framework of the SM, and therefore offer a unique opportunity to search for unknown processes, for instance non-SM couplings to yet undiscovered charged partners of the Higgs boson [6] or hypothetical leptoquarks [7]. Such searches have been performed on data collected by three different experiments, BABAR and Belle at e^+e^- colliders in the U.S.A. and in Japan, and LHCb at the proton-proton (pp) collider at CERN in Europe.

In the following, details of the measurements, their results and preliminary studies to understand the observed effects will be presented, along with prospects for improved sensitivity and complementary measurements. This article is partially based on an earlier review with the same title [8].

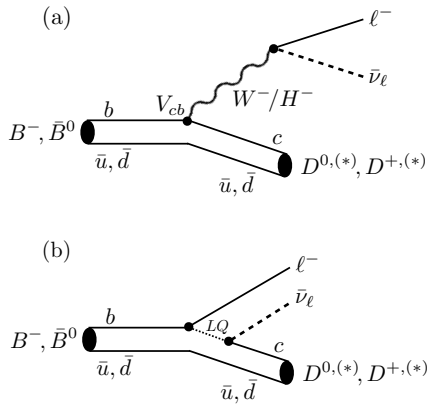


Fig. 1 Diagrams for decay process for $\bar{B} \rightarrow D^{(*)} \ell^- \bar{\nu}_\ell$ decays: (a) for a tree level process mediated either by a vector boson (W^-) or a hypothetical spin-0 charged Higgs boson (H^-), or (b) couplings to a hypothetical lepto-quark (LQ).

Standard Model Predictions of B Meson Decay Rates

According to the SM, semileptonic decays of B mesons are mediated by the W^- boson, as shown schematically in Figure 1a. The differential decay rate, $d\Gamma$, for semileptonic decays involving $D^{(*)}$ mesons depends on both m_ℓ^2 and q^2 , the invariant mass squared of the lepton pair [9],

$$\frac{d\Gamma^{SM}(\bar{B} \rightarrow D^{(*)} \ell^- \bar{\nu}_\ell)}{dq^2} = \underbrace{\frac{G_F^2 |V_{cb}|^2 |\mathbf{p}_{D^{(*)}}^*|^2}{96\pi^3 m_B^2} \left(1 - \frac{m_\ell^2}{q^2}\right)^2}_{\text{universal and phase space factors}} \underbrace{\left[(|H_+|^2 + |H_-|^2 + |H_0|^2) \left(1 + \frac{m_\ell^2}{2q^2}\right) + \frac{3m_\ell^2}{2q^2} |H_s|^2 \right]}_{\text{hadronic effects}}. \quad (1)$$

The first factor is universal for all semileptonic B decays, containing a quark flavor mixing parameter [10] $|V_{cb}|$ [11] for $b \rightarrow c$ quark transitions, and $p_{D^{(*)}}^*$, the 3-momentum of the $D^{(*)}$ meson. The four helicity [12] amplitudes H_+ , H_- , H_0 and H_s capture the impact of hadronic effects. They depend on the spin of the charm meson and on q^2 . The much larger τ mass not only impacts the rate, but also the decay kinematics via the H_s amplitude. All four amplitudes contribute to $\bar{B} \rightarrow D^{(*)} \ell^- \bar{\nu}_\ell$, while only H_0 and H_s contribute to $\bar{B} \rightarrow D \ell^- \bar{\nu}_\ell$, which leads to a higher sensitivity of this decay mode to the scalar contribution H_s . The minimum value of q^2 is equal to m_ℓ^2 .

Measurements of the ratios of semileptonic branching fractions remove the dependence on $|V_{cb}|$, lead to a partial cancellation of theoretical uncertainties related

to hadronic effects, and reduce of the impact of experimental uncertainties. The averages of the current predictions [13,14] and [14,15,16] for the two ratios are

$$\mathcal{R}_D^{SM} = \frac{\mathcal{B}(\bar{B} \rightarrow D \tau^- \bar{\nu}_\tau)}{\mathcal{B}(\bar{B} \rightarrow D e^- \bar{\nu}_e)} = 0.299 \pm 0.003 \quad (2)$$

$$\mathcal{R}_{D^*}^{SM} = \frac{\mathcal{B}(\bar{B} \rightarrow D^* \tau^- \bar{\nu}_\tau)}{\mathcal{B}(\bar{B} \rightarrow D^* e^- \bar{\nu}_e)} = 0.258 \pm 0.005. \quad (3)$$

The predicted ratios for $\mathcal{B}(\bar{B} \rightarrow D^{(*)} \mu^- \bar{\nu}_\mu)$ are identical within the quoted precision. In the following, $\bar{B} \rightarrow D^{(*)} \tau^- \bar{\nu}_\tau$ decays are referred to as the "signal", and $\bar{B} \rightarrow D^{(*)} e^- \bar{\nu}_e$ with $\ell = e, \mu$ are referred to as "normalization".

B Meson Production and Detection

B meson decays have been studied at pp and e^+e^- colliding beam facilities, operating at very different beam energies.

The e^+e^- colliders operated at a fixed energy of 10.579 GeV in the years 1999 to 2010. At this energy, about 20 MeV above the kinematic threshold for $B\bar{B}$ production, e^+ and e^- annihilate and produce a particle, commonly referred to as $\Upsilon(4S)$, which decays almost exclusively to B^+B^- or $B^0\bar{B}^0$ pairs. The maximum production rate for these $\Upsilon(4S) \rightarrow B\bar{B}$ events of 20 Hz was achieved at KEK, compared to the multi-hadron non- $B\bar{B}$ background rate of about 80 Hz.

B mesons have very low momenta, ≈ 300 MeV, and therefore their decay products are distributed almost isotropically in the detector. The BABAR [17,18] and Belle [19] detectors were designed to cover close to 90% of the total solid angle, thereby enabling the reconstruction of almost all final state particles from decays of the two B mesons, except neutrinos.

The LHC pp collider operated at total energies of 7 and 8 TeV from 2008 to 2012. In inelastic pp collisions, high energy gluons, the carriers of the strong force, produce pairs of B hadrons (mesons or baryons) along with a large number of other charged and neutral particles, in roughly 1% of the pp interactions. The B hadrons are typically produced at small angles to the beam and with high momenta, features that determined the design of the LHCb detector [20,21], a single arm forward spectrometer, covering the polar angle range of 3 – 23 degrees.

The high momentum and relatively long B hadron lifetimes result in decay distances of several cm. Very precise measurements of the pp interaction point, combined with the detection of charged particle trajectories from B , D and τ decay vertices are the very effective method to separate B decays from background.

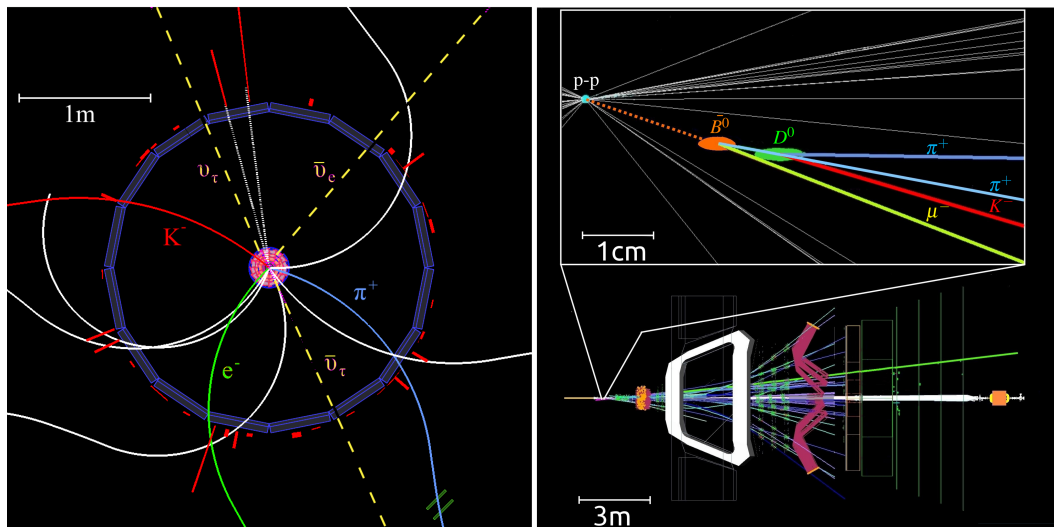


Fig. 2 Belle (a) and LHCb (b) single event displays: Trajectories of charged particles are shown as colored solid lines, energy deposits in the calorimeters are depicted by red bars. The Belle display is an end view perpendicular to the beam axis with the silicon detector in the center (small orange circle) and the Cherenkov detectors (purple polygon). This is a $\Upsilon(4S) \rightarrow B^+B^-$ event, with $B^- \rightarrow D^0\tau^-\bar{\nu}_\tau$, $D^0 \rightarrow K^-\pi^+$ and $\tau^- \rightarrow e^-\nu_\tau\bar{\nu}_e$, and the B^+ decaying to five charged particles (white solid lines) and two photons. The trajectories of undetected neutrinos are marked as dashed yellow lines. The LHCb display is a side view with the proton beams indicated as a white horizontal line with the interaction point far to the left, followed by the dipole magnet (white trapezoid) and the Cherenkov detector (red lines). The area close to the interaction point is enlarged above, showing the tracks of the charged particles produced in the pp interaction, the B^0 path (dotted orange line), and its decay $B^0 \rightarrow D^{*+}\tau^-\bar{\nu}_\tau$ with $D^{*+} \rightarrow D^0\pi^+$ and $D^0 \rightarrow K^-\pi^+$, plus the μ^- from the decay of a very short-lived τ^- .

All three experiments rely on layers of finely segmented silicon strip detectors to locate the beam-beam interaction point and decay vertices of long-lived particles. A combination of silicon strip detectors and multiple layers of gaseous detectors measure the trajectories of charged particles deflected in a magnetic field. Devices which sense Cherenkov radiation distinguish charged particles of different masses, and arrays of cesium iodide crystals measure the energy of photons and identify electrons at BABAR and Belle. Muons are identified as particles penetrating a stack of steel absorbers interleaved with large area gaseous detectors. Examples of reconstructed signal events recorded by the Belle and LHCb experiments are shown in Figure 2.

BABAR and Belle exploit the $B\bar{B}$ pair production at the $\Upsilon(4S)$ resonance and have independently developed two sets of algorithms to tag $B\bar{B}$ events by reconstructing a hadronic or semileptonic decay of one of the two B mesons, referred to as B_{tag} . The hadronic tag algorithms [22, 23] search for the best match between one of more than a thousand possible decay chains and a subset of all detected particles in the event. The efficiency for finding a correctly matched B_{tag} is unfortunately small, typically 0.3%. The semileptonic tag algorithms relies on a few decays modes with larger branching fractions, resulting in an efficiency of about 1%. However, the presence of the neutrino leads to weaker

constraints on the B_{tag} and more importantly on the signal B decay.

Measurements of $\bar{B} \rightarrow D^{(*)}\tau^-\bar{\nu}_\tau$ Decays

The BABAR and Belle event selection required a B_{tag} , plus a D or D^* meson, and a charged lepton $\ell^- = e^-$ or μ^- . Charged and neutral D mesons are reconstructed from combinations of pions and kaons with invariant masses compatible with the D meson mass. The higher-mass D^{*0} and D^{*+} mesons are identified by their $D^* \rightarrow D\pi$ and $D^* \rightarrow D\gamma$ decays. Non- $B\bar{B}$ backgrounds and misreconstructed events are greatly suppressed by the B_{tag} reconstruction. The remaining background is further reduced by multivariate selections.

At LHCb, only decays of \bar{B}^0 mesons producing a D^{*+} meson and a μ^- are selected. The D^{*+} meson is reconstructed exclusively in $D^{*+} \rightarrow D^0(\rightarrow K^-\pi^+)\pi^+$ decays. The use of a single decay chain significantly simplifies this analysis and the reduced efficiency is compensated by the very large production rate of B mesons at the LHC. The bulk of the background is rejected by requiring that all charged particles from the B candidate (and no other tracks) originate from a common vertex that is significantly separated from the pp collision point.

While for BABAR and Belle the B momentum is fixed and known precisely, for LHCb the direction of the B momentum is inferred from the reconstructed pp collision point and $D^{*+}\mu^-$ vertex, and the magnitude of the B momentum is estimated by equating its component parallel to the beam axis to that of the $D^{*+}\mu^-$ combination, rescaled by the ratio of the B mass to the measured $D^{*+}\mu^-$ mass.

The yields for the signal and normalization B decays, and various background contributions are determined by maximum likelihood fits to the observed data distributions. All three experiments rely on three variables: The invariant mass squared of all undetected particles, $m_{\text{miss}}^2 = E_{\text{miss}}^2 - \mathbf{p}_{\text{miss}}^2$, E_ℓ^* , the energy of the charged lepton in the B rest frame, and q^2 , the invariant mass squared of the lepton pair. E_{miss} and \mathbf{p}_{miss} refer to the missing energy and momentum of the B meson. BABAR and Belle restrict the data to $q^2 > 4 \text{ GeV}^2$ to enhance the contribution from signal decays. Control samples are used to validate the simulated distributions and constrain the size and kinematic features of the background contributions.

BABAR performs the 2D fit, whereas LHCb divides the q^2 range into four intervals, thus performing a fully 3D fit. Belle combined two 1D fits, 1) to the m_{miss}^2 distribution in the low m_{miss}^2 region ($m_{\text{miss}}^2 < 0.85 \text{ GeV}^2$) dominated by the normalization decays, and 2) to a multivariate classifier for data in the high m_{miss}^2 region.

Figure 3 shows one-dimensional projections of the data and the fitted contributions from signal and normalization B decays, and various backgrounds. The m_{miss}^2 distributions for BABAR (and likewise for Belle) show a narrow peak at zero (Figure 3 a,d), dominated by normalization decays with a single neutrino, whereas the signal events with three neutrinos extend to about 10 GeV^2 . For $\bar{B} \rightarrow D\ell^-\bar{\nu}_\ell$ decays, there is a sizable contribution from $\bar{B} \rightarrow D^*\ell^-\bar{\nu}_\ell$ decays, for which the pion or photon from the $D^* \rightarrow D\pi$ or $D^* \rightarrow D\gamma$ decay was not reconstructed. For LHCb, the peak at zero is somewhat broader and has a long tail into the signal region (Figure 3 h) because of uncertainties in the estimation of the B_{sig} momentum. The E_ℓ^* distributions (Figure 3 c,f,i) provide additional discrimination, since a lepton from a normalization decay has a higher average momentum than a lepton originating from secondary $\tau^- \rightarrow \ell^-\nu_\tau\bar{\nu}_\ell$ decays.

Among the background contributions, semileptonic B decays to the higher mass D^{**} mesons are of concern, primarily because their branching fractions and form factors are not well known. These D^{**} states decay to a D or D^* meson plus additional low energy particles which, if not reconstructed, have a broader m_{miss}^2 distribution. They can be distinguished from signal decays

by their E_ℓ^* distributions which extend to higher values. At LHCb, an important background arises from $B \rightarrow D^{(*)}H_cX$ decays, where H_c is a charm hadron decaying either leptonically or semileptonically, and X refers to additional low mass hadrons, if present. These decays produce m_{miss}^2 and E_ℓ^* spectra that are similar to those of signal events (Figure 3 h,i).

LHCb recently reported a measurement of the ratio $\mathcal{R}_{D^{*+}}$ using $\tau^- \rightarrow \pi^-\pi^+\pi^-(\pi^0)\bar{\nu}_\tau$ decays [25]. By requiring a 4σ separation of the 3-prong vertex from the B decay vertex, 99% of the $B^0 \rightarrow D^{*+}\pi^-\pi^+\pi^-(\pi^0)$ background is removed, while 34% of the signal is retained, and the purity of the signal sample improved by a factor of four compared to the purely leptonic τ^- decay.

The signal yield is extracted via binned fit to a 3D distribution for τ decay time (based on the estimated 3-pion momentum), and q^2 , in 4 bins of the output of the BTD (Boosted Decision Tree) algorithm employed to suppress various backgrounds. Figure 4 shows the projections of the three distributions, resulting in a yield of (1296 ± 86) signal events. This rate is normalized to a much larger sample of $\bar{B}^0 \rightarrow D^{*+}\pi^-\pi^+\pi^-$ decays. Correcting for efficiencies and the τ branching fraction, this translates to

$$\mathcal{K} \equiv \frac{\mathcal{B}(\bar{B}^0 \rightarrow D^{*+}\tau^-\bar{\nu}_\tau)}{\mathcal{B}(\bar{B}^0 \rightarrow D^{*+}(3\pi)^-)} = 1.97 \pm 0.137_{\text{stat}} \pm 0.18_{\text{syst}}.$$

Taking into account the averages of measurements of the two branching fractions, LHCb quotes

$$\begin{aligned} \mathcal{R}_{D^{*+}} &= \mathcal{K} \times \frac{\mathcal{B}(\bar{B}^0 \rightarrow D^{*+}(3\pi)^-)}{\mathcal{B}(\bar{B}^0 \rightarrow D^{*+}\mu^-\bar{\nu}_\tau)} \\ &= 0.291 \pm 0.019_{\text{stat}} \pm 0.026_{\text{syst}} \pm 0.013_{\text{ext}}. \end{aligned} \quad (4)$$

With much larger future data and MC samples this method holds great promise for future analyses exploiting the 3-prong τ decay vertex.

Figure 5 shows the measured values for \mathcal{R}_D and \mathcal{R}_{D^*} by BABAR [23] (including a more recent measurement using $\tau^+ \rightarrow h^+\nu_\tau$ decays, where h^+ refers to a π^+ or ρ^+), and LHCb [24,25]. The averages of the measurements [28] are

$$\mathcal{R}_D = 0.407 \pm 0.039_{\text{stat}} \pm 0.024_{\text{syst}}, \quad (5)$$

$$\mathcal{R}_{D^*} = 0.306 \pm 0.013_{\text{stat}} \pm 0.007_{\text{syst}}. \quad (6)$$

Both values exceed the SM expectations. Taking into account the correlations, the combined difference between the measured and expected values has a significance of close to four standard deviations.

Interpretations of Results

The results presented here have attracted the attention of the physics community and have resulted in several

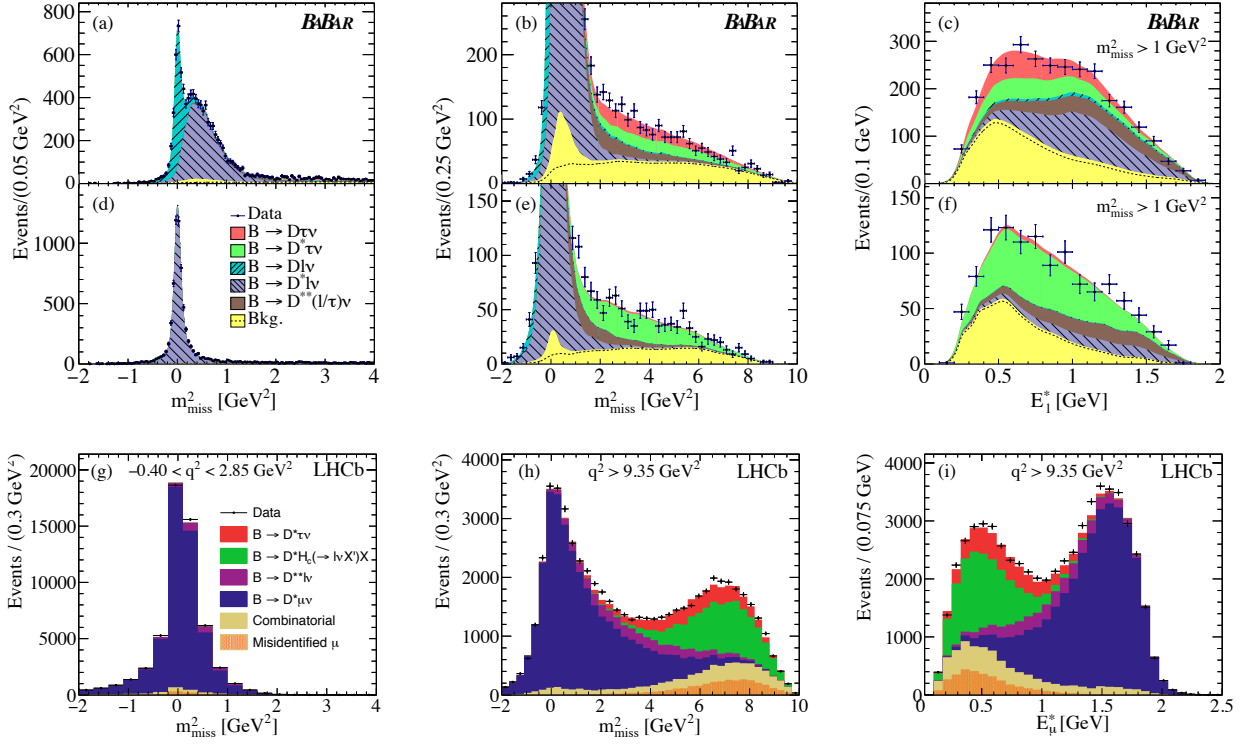


Fig. 3 Extraction of the ratios \mathcal{R}_D and \mathcal{R}_{D^*} by maximum likelihood fits: Comparison of the projections of the measured m_{miss}^2 and E_ℓ^* distributions (data points) and the fitted distributions of signal and background contributions for the BABAR fit [23] to the $D\ell$ samples (a-c) and $D^*\ell$ samples (d-f), as well the LHCb fit [24] to the $D^{*+}\ell$ sample (g-i). The E_ℓ^* distributions in (c) and (f) are signal enhanced by the restriction $m_{\text{miss}}^2 > 1 \text{ GeV}^2$. The LHCb results are presented for two different q^2 intervals, the lowest, which is free of $B^0 \rightarrow D^{*+}\tau^-\bar{\nu}_\tau$ decays (g), and the highest where this contribution is large (h,i).

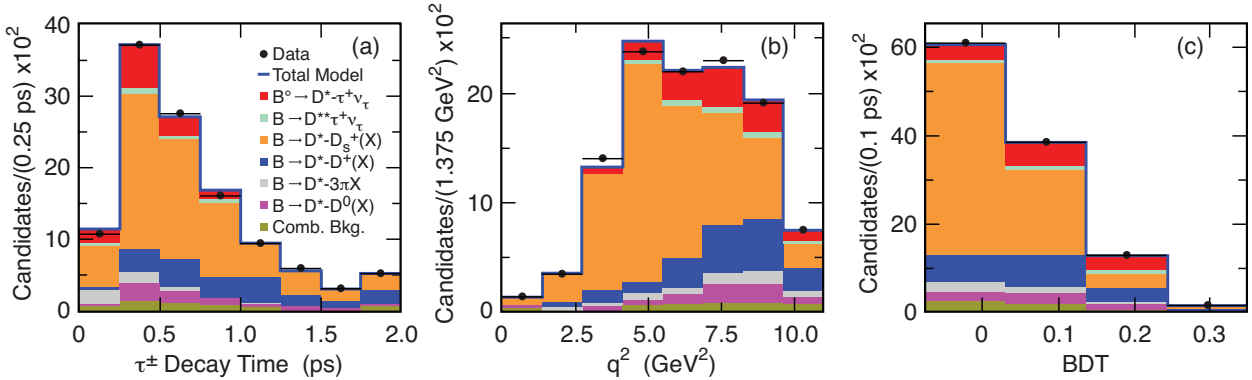


Fig. 4 LHCb extraction of the $B \rightarrow D^{(*)}\tau^-\bar{\nu}_\tau$ decays with 3-prong τ vertices by a 3D maximum likelihood fit: Projections of distributions of the three variables showing the dominant backgrounds from $B \rightarrow D^{(*)}H_cX$ decays [25].

potential explanations of this apparent violation of lepton universality in B decays involving the τ lepton.

Among the simplest explanations for these observed rate increases for decays involving τ^- would be the existence of a new vector boson, W'^- , similar to the SM W^- boson, but of greater mass, and with couplings of varying strengths to different leptons and quarks. This could lead to changes in \mathcal{R}_D and \mathcal{R}_{D^*} , but not in the kinematics of the decays. However, this option is con-

strained by searches for $W'^- \rightarrow t\bar{b}$ decays [32,33] at the LHC collider at CERN, as well as by precision measurements of μ [34] and τ [35] decays.

Another potentially interesting candidate would be a new type of Higgs boson, a particle of spin 0, similar to the recently discovered neutral Higgs [36,37], but electrically charged. This charged Higgs (H^-) was proposed in minimal extensions of the SM [38], which are part of broader theoretical frameworks such as super-

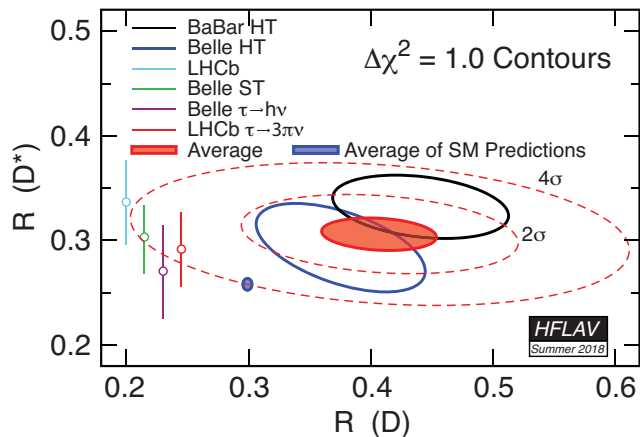


Fig. 5 Results from BABAR [23], Belle [26,27], and LHCb [24,25]: Their values and 1σ contours. The average calculated by the Heavy Flavor Averaging Group [28] is compared to SM predictions [29,30,31]. HT and ST refer to hadronic and semileptonic tag analyses.

symmetry [39]. The H^- would mediate weak decays, similar to the W^- (as indicated in Figure 1), but couple differently to leptons of different mass. The q^2 and angular distributions would be impacted because of the different spin of the H^- .

Another feasible solution might be leptoquarks [40], hypothetical particles with both electric and color (strong) charges that allow transitions from quarks to leptons and vice versa, and offer a unified description of three generations of quarks and leptons. Among the ten different types of leptoquarks, six could contribute to $B \rightarrow D^{(*)}\tau\nu$ decays [7]. A diagram of a spin-0 state mediating quark-lepton transitions is shown in Figure 1b for the B decay modes under study.

BABAR and Belle have studied the implications of these hypothetical particles in the context of specific models [23,26]. The measured values of \mathcal{R}_D and \mathcal{R}_{D^*} do not support the simplest of the two-Higgs doublet models (type II), however, more general Higgs models with appropriate parameter choices can accommodate the measured ratios [41,42,43]. Some of the leptoquark models could also explain the measured values of \mathcal{R}_D and \mathcal{R}_{D^*} [44,45,46], evading constraints from direct searches of leptoquarks in ep collisions [47] at HERA [48,49] and pp collisions at LHC [50,51].

The kinematics of $B \rightarrow D^{(*)}\tau\nu$ decays should permit further discrimination of new physics scenarios based on the decay distributions of final state particles. The q^2 spectrum [23,26] and the momentum distributions of the $D^{(*)}$ and electron or muon [27] have been examined. Within the current experimental uncertainties, the observed shapes of these distributions are consistent with SM predictions.

Conclusions and Outlook

While the observed enhancements of the semileptonic B meson decay rates involving a τ lepton relative to the expectations of the SM of electroweak interactions are intriguing, their significance is not sufficient to unambiguously establish a violation of lepton universality at this time. However, the fact that these unexpected enhancements have been observed by three experiments operating in very different environments deserves further attention.

At present, the measurements are limited by the size of the available data samples and uncertainties in the reconstruction efficiencies and background estimates. It is not inconceivable that the experiments have underestimated these uncertainties, or missed a more conventional explanation. Furthermore, while it is very unlikely, it cannot be totally excluded that the theoretical SM predictions are not as firm as presently assumed. Currently, the experimenters are continuing their analysis efforts, refining their methods, enhancing the signal samples by adding additional decay modes, improving the efficiency and selectivity of the tagging algorithms, as well as the Monte Carlo simulations, and scrutinizing all other aspects of the signal extraction.

At KEK, the e^+e^- collider has undergone major upgrades and is expected to enlarge the data sample by close to a factor of 40 over a period of about ten or more years. In parallel, the Belle detector has also been substantially upgraded, and following commissioning Belle II is expected to be in full operation a year from now.

The much larger event samples should lead to more precise measurements $B \rightarrow D^{(*)}\tau\nu$ decays, based on detailed studies of their kinematics, i.e. q^2 and angular distributions, as well as the τ polarization in $B \rightarrow D^*\tau\nu$ decays. The feasibility of such a measurement has recently been demonstrated [52]. The first measurements of $\mathcal{R}_{D^{**}}$ [53] should lead to a significant reduction of the uncertainties in the estimate of this background for $\mathcal{R}_{D^{(*)}}$ measurements. Belle analyses will be critical to improved understanding of form factors for various semileptonic B and D meson decays.

The unique capabilities of Belle II should allow studies of inclusive semileptonic decays, like $B \rightarrow X_u\ell^+\nu_\tau$ ($\ell = e, \mu, \tau$) for both charged and neutral B decays; X_u refers to the sum of non-charm states X_u . The larger data samples and developments of more refined tagging algorithms will benefit many analyses, in particular $B^- \rightarrow \tau^-\bar{\nu}_\tau$ decays, should lead to significant reductions in statistical uncertainties and thus allow more stringent tests of SM predictions for these purely leptonic B meson decays.

By the end of 2018, the accumulated LHCb data sample is expected to increase by a factor of three. In the near future, LHCb will complete several important analyses, among them their first measurement of the $\bar{B} \rightarrow D\tau^-\bar{\nu}_\tau$ decay, which will also improve results for $\bar{B} \rightarrow D^*\tau^-\bar{\nu}_\tau$. In parallel, samples with the $\tau^- \rightarrow \pi^-\pi^+\pi^-\nu_\tau$ decay mode will be used to improve the signal purity.

In the longer term future, LHCb is planning to further enhance the trigger selection and data rate capability to record much larger event samples.

Given the large production rate of B_s and B_c mesons and various B baryons, LHCb is planning a broad program to measure their semileptonic branching fractions and form factors and to search for deviation for SM expectations. For instance, $B_s^0 \rightarrow D_s^-\tau^+\nu_\tau$ decays which probe the same interaction as R_D . LHCb recently observed the decay $B_c^+ \rightarrow J/\psi\tau^+\nu_\tau$ resulting in a final state of 3 muons and three neutrinos, and measured the ratio $\mathcal{R}_{J/\psi} = 0.71 \pm 0.17_{stat} \pm 0.18_{sys}$ [54]. At present, the uncertainties are dominated by the very small signal and the limited knowledge of the form factor.

Measurements of semileptonic A_b decays probe different spin structures, specifically the favored $b \rightarrow c$ transition $A_b^0 \rightarrow A_c^+\tau^-\bar{\nu}_\tau$ and the suppressed $b \rightarrow u$ transition $A_b^0 \rightarrow p\tau^-\bar{\nu}_\tau$ measurements that are expected to distinguish between interpretations. Other $b \rightarrow u$ transitions, like $B^+ \rightarrow \rho^0\tau^-\nu_\tau$ or $B^+ \rightarrow p\bar{p}\tau^+\nu_\tau$ are also considered.

Independently, several experiments have examined decay rates and angular distributions for four B^+ decays, $B^+ \rightarrow K^{(*)+}\mu^+\mu^-$ and $B^+ \rightarrow K^{(*)+}e^+e^-$. In the framework of the SM, these decays are very rare, since they involve $b \rightarrow s$ quark transitions. LHCb [55] published a measurement of the ratio,

$$\mathcal{R}_K = \frac{\mathcal{B}(B^+ \rightarrow K^{(*)+}\mu^+\mu^-)}{\mathcal{B}(B^+ \rightarrow K^{(*)+}e^+e^-)} = 0.745 \pm_{0.074}^{0.090} \pm 0.036. \quad (7)$$

This result is 2.6 standard deviations smaller than the SM expectation of about 1.0. Some theoretical new types of interactions could explain this result. For instance, leptoquarks can mediate this decay and result in higher rates for electrons than muons [56, 57]. BABAR [58], LHCb [59] and Belle [60] have analyzed angular distributions for the four decay modes and observed general agreement with SM predictions, except for local deviations, the most significant by LHCb at the level of 3.4 standard deviations. Again, more data are needed to enhance the significance and find possible links to B decays involving τ leptons.

In conclusion, we can expect much larger event samples from the LHCb and Belle II experiments in the not

too distant future. These data will be critical to the effort to understand whether the tantalizing results obtained to date are an early indication of beyond-the-SM physics processes or the result of larger-than-expected statistical or systematic deviations. A confirmation of new physics contributions in these decays would shake the foundations of our understanding of matter and trigger an intense program of experimental and theoretical research.

References

1. R. B. Mann. *An introduction to particle physics and the Standard Model*. CRC Press, New York, NY (USA), 2010.
2. S. Weinberg. *The quantum theory of fields. Vol. 2: Modern applications*. Cambridge University Press, Cambridge (UK), 2013.
3. M. Ablikim et al. Precision measurement of the mass of the τ lepton. *Phys. Rev.*, D90:012001, 2014.
4. C. Lazzeroni et al. Precision measurement of the ratio of the charged kaon leptonic decay rates. *Phys. Lett.*, B719:326–336, 2013.
5. Unless stated otherwise, the inclusion of charged-conjugate states and decay modes is implied here and in the following.
6. M. Tanaka. Charged Higgs effects on exclusive semitauonic B decays. *Z. Phys.*, C67:321–326, 1995.
7. M. Freytsis, Z. Ligeti, and J. T. Ruderman. Flavor models for $\bar{B} \rightarrow D^{(*)}\tau\bar{\nu}$. *Phys. Rev.*, D92:054018, 2015.
8. G. Ciezarek, M. Franco Sevilla, B. Hamilton, R. Kowalewski, T. Kuhr, V. Lüth, and Y. Sato. A challenge to lepton universality in B-meson decays. *Nature*, 546:227, 2017.
9. J. G. Korner and G. A. Schuler. Exclusive semileptonic heavy meson decays including lepton mass effects. *Z. Phys.*, C46:93, 1990.
10. M. Kobayashi and T. Maskawa. CP violation in the renormalizable theory of weak interaction. *Prog. Theor. Phys.*, 49:652–657, 1973.
11. Y. Amhis et al. Averages of b -hadron, c -hadron, and τ -lepton properties. arXiv:1412.7515, 2014.
12. Helicity refers to the component of the angular momentum of a particle parallel to the direction to its momentum.
13. Dante Bigi and Paolo Gambino. Revisiting $B \rightarrow D\ell\nu$. *Phys. Rev.*, D94(9):094008, 2016.
14. Florian U. Bernlochner, Zoltan Ligeti, Michele Papucci, and Dean J. Robinson. Combined analysis of semileptonic B decays to D and D^* : $R(D^{(*)})$, $|V_{cb}|$, and new physics. *Phys. Rev.*, D95(11):115008, 2017. [Erratum: *Phys. Rev. D*97,no.5,059902(2018)].
15. Dante Bigi, Paolo Gambino, and Stefan Schacht. $R(D^*)$, $|V_{cb}|$, and the Heavy Quark Symmetry relations between form factors. *JHEP*, 11:061, 2017.
16. Sneha Jaiswal, Soumitra Nandi, and Sunando Kumar Patra. Extraction of $|V_{cb}|$ from $B \rightarrow D^{(*)}\ell\nu_\ell$ and the Standard Model predictions of $R(D^{(*)})$. *JHEP*, 12:060, 2017.
17. B. Aubert et al. The BABAR detector. *Nucl. Instrum. Meth.*, A479:1–116, 2002.
18. B. Aubert et al. The BABAR detector: upgrades, operation and performance. *Nucl. Instrum. Meth.*, A729:615–701, 2013.

19. A. Abashian et al. The Belle detector. *Nucl. Instrum. Meth.*, A479:117–232, 2002.
20. A. A. Alves, Jr. et al. The LHCb detector at the LHC. *JINST*, 3:S08005, 2008.
21. F. Dettori. Performance of the LHCb detector during the LHC proton runs 2010-2012. *Nucl. Instrum. Meth.*, A732:40–43, 2013.
22. M. Feindt et al. A hierarchical neuroBayes-based algorithm for full reconstruction of B mesons at B factories. *Nucl. Instrum. Meth.*, A654:432–440, 2011.
23. J. P. Lees et al. Measurement of an excess of $\bar{B} \rightarrow D^{(*)}\tau^-\bar{\nu}_\tau$ decays and Implications for charged Higgs bosons. *Phys. Rev.*, D88:072012, 2013.
24. R. Aaij et al. Measurement of the ratio of branching fractions $\mathcal{B}(\bar{B}^0 \rightarrow D^{*+}\tau^-\bar{\nu}_\tau)/\mathcal{B}(\bar{B}^0 \rightarrow D^{*+}\mu^-\bar{\nu}_\mu)$. *Phys. Rev. Lett.*, 115:111803, 2015. [Addendum: *Phys. Rev. Lett.*115,no.15,159901(2015)].
25. R. Aaij et al. Test of Lepton Flavor Universality by the measurement of the $B^0 \rightarrow D^{*+}\tau^+\nu_\tau$ branching fraction using three-prong τ decays. *Phys. Rev.*, D97(7):072013, 2018.
26. M. Huschle et al. Measurement of the branching ratio of $\bar{B} \rightarrow D^{(*)}\tau^-\bar{\nu}_\tau$ relative to $\bar{B} \rightarrow D^{(*)}\ell^-\bar{\nu}_\ell$ decays with hadronic tagging at Belle. *Phys. Rev.*, D92:072014, 2015.
27. Y. Sato et al. Measurement of the branching ratio of $\bar{B}^0 \rightarrow D^{*+}\tau^-\bar{\nu}_\tau$ relative to $\bar{B}^0 \rightarrow D^{*+}\ell^-\bar{\nu}_\ell$ decays with semileptonic tagging. *Phys. Rev.*, D94:072007, 2016.
28. Heavy Flavor Averaging Group. Average of \mathcal{R}_D and \mathcal{R}_{D^*} for Summer 2018. <https://hflav-eos.web.cern.ch/hflav-eos/semi/summer18/RDRDs.html>, 2018.
29. H. Na et al. $B \rightarrow D\ell\nu$ form factors at nonzero recoil and extraction of $|V_{cb}|$. *Phys. Rev.*, D92:054510, 2015. [Erratum: *Phys. Rev.*D93,119906(2016)].
30. S. Fajfer, J. F. Kamenik, and I. Nisandzic. On the $B \rightarrow D^*\tau\bar{\nu}_\tau$ sensitivity to new physics. *Phys. Rev.*, D85:094025, 2012.
31. J. A. Bailey et al. $B \rightarrow D\ell\nu$ form factors at nonzero recoil and $|V_{cb}|$ from 2+1-flavor lattice QCD. *Phys. Rev. D*, 92(3):034506, 2015.
32. S. Chatrchyan et al. Search for a W' boson decaying to a bottom quark and a top quark in pp collisions at $\sqrt{s} = 7$ TeV. *Phys. Lett.*, B718:1229–1251, 2013.
33. G. Aad et al. Search for $W' \rightarrow tb$ in the lepton plus jets final state in proton-proton collisions at a centre-of-mass energy of $\sqrt{s} = 8$ TeV with the ATLAS detector. *Phys. Lett.*, B743:235–255, 2015.
34. R. Prieels et al. Measurement of the parameter ξ'' in polarized muon decay and implications on exotic couplings of the leptonic weak interaction. *Phys. Rev.*, D90(11):112003, 2014.
35. A. Stahl. Physics with tau leptons. *Springer Tracts Mod. Phys.*, 160:1–316, 2000.
36. S. Chatrchyan et al. Observation of a new boson at a mass of 125 GeV with the CMS experiment at the LHC. *Phys. Lett.*, B716:30, 2012.
37. G. Aad et al. Observation of a new particle in the search for the Standard Model Higgs boson with the ATLAS detector at the LHC. *Phys. Lett.*, B716:1, 2012.
38. V. D. Barger, J. L. Hewett, and R. J. N. Phillips. New constraints on the charged Higgs sector in Two-Higgs-Doublet Models. *Phys. Rev.*, D41:3421–3441, 1990.
39. J. F. Gunion and H. E. Haber. Higgs Bosons in supersymmetric models. 1. *Nucl. Phys.*, B272:1, 1986. [Erratum: *Nucl. Phys.*B402,567(1993)].
40. I. Dorsner, S. Fajfer, A. Greljo, J. F. Kamenik, and N. Kosnik. Physics of leptoquarks in precision experiments and at particle colliders. *Phys. Rept.*, 641:1–68, 2016.
41. A. Datta, M. Duraisamy, and D. Ghosh. Diagnosing new physics in $b \rightarrow c\tau\nu_\tau$ decays in the light of the recent BABAR result. *Phys. Rev.*, D86:034027, 2012.
42. A. Crivellin, C. Greub, and A. Kokulu. Explaining $B \rightarrow D\tau\nu$, $B \rightarrow D^*\tau\nu$ and $B \rightarrow \tau\nu$ in a 2HDM of type III. *Phys. Rev.*, D86:054014, 2012.
43. S. Fajfer, J. F. Kamenik, I. Nisandzic, and J. Zupan. Implications of lepton flavor universality Violations in B decays. *Phys. Rev. Lett.*, 109:161801, 2012.
44. Y. Sakaki, A. Tanaka, M. Tayduganov, and R. Watanabe. Testing leptoquark models in $\bar{B} \rightarrow D^{(*)}\tau\bar{\nu}$. *Phys. Rev.*, D88:094012, 2013.
45. B. Dumont, K. Nishiwaki, and R. Watanabe. LHC constraints and prospects for S_1 scalar leptoquark explaining the $\bar{B} \rightarrow D^{(*)}\tau\bar{\nu}$ anomaly. *Phys. Rev.*, D94:034001, 2016.
46. M. Bauer and M. Neubert. Minimal leptoquark explanation for the $R_{D^{(*)}}$, R_K , and $(g-2)_g$ anomalies. *Phys. Rev. Lett.*, 116(14):141802, 2016.
47. W. Buchmuller, R. Ruckl, and D. Wyler. Leptoquarks in lepton - quark collisions. *Phys. Lett.*, B191:442–448, 1987. [Erratum: *Phys. Lett.*B448,320(1999)].
48. S. Chekanov et al. A Search for resonance decays to lepton + jet at HERA and limits on leptoquarks. *Phys. Rev.*, D68:052004, 2003.
49. F. D. Aaron et al. Search for first generation leptoquarks in ep collisions at HERA. *Phys. Lett.*, B704:388–396, 2011.
50. G. Aad et al. Search for third generation scalar leptoquarks in pp collisions at $\sqrt{s} = 7$ TeV with the ATLAS detector. *JHEP*, 06:033, 2013.
51. V. Khachatryan et al. Search for pair production of third-generation scalar leptoquarks and top squarks in pp collisions at $\sqrt{s} = 8$ TeV. *Phys. Lett.*, B739:229–249, 2014.
52. S. Hirose et al. Measurement of the τ lepton polarization and $R(D^*)$ in the decay $\bar{B} \rightarrow D^*\tau^-\bar{\nu}_\tau$. arXiv:1612.00529, 2016.
53. A. Vossen et al. Measurement of the branching fraction of $B \rightarrow D^{(*)}\pi\ell\nu$ at Belle using hadronic tagging in fully reconstructed events. 2018.
54. R. Aaij et al. Measurement of the ratio of branching fractions $\mathcal{B}(B_c^+ \rightarrow J/\psi\tau^+\nu_\tau)/\mathcal{B}(B_c^+ \rightarrow J/\psi\mu^+\nu_\mu)$. *Phys. Rev. Lett.*, 120(12):121801, 2018.
55. R. Aaij et al. Test of lepton universality using $B^+ \rightarrow K^+\ell^+\ell^-$ decays. *Phys. Rev. Lett.*, 113:151601, 2014.
56. G. Hiller and M. Schmaltz. R_K and future $b \rightarrow s\ell\ell$ physics beyond the standard model opportunities. *Phys. Rev.*, D90:054014, 2014.
57. D. Bećirević, S. Fajfer, N. Košnik, and S. Olcyr. Leptoquark model to explain the B -physics anomalies, R_K and R_D . *Phys. Rev. D*, 94(11):115021, 2016.
58. J. P. Lees et al. Measurement of branching fractions and rate asymmetries in the rare Decays $B \rightarrow K^{(*)}l^+l^-$. *Phys. Rev.*, D86:032012, 2012.
59. R. Aaij et al. Angular analysis of the $B^0 \rightarrow K^{*0}\mu^+\mu^-$ decay using 3 fb^{-1} of integrated luminosity. *JHEP*, 1602:104, 2016.
60. S. Wehle et al. Lepton-flavor-dependent angular analysis of $B \rightarrow K^*\ell^+\ell^-$. arXiv:1612.05014, 2016.